



Research article

Research on wind deflection risk early warning method of transmission line driven by digital twin and data fusion

Wulue Zheng*, Qingpeng Chen, Xin Zhang, Wenjun Yuan and Hao Chen

China Southern Power Grid Extra High Voltage Power Transmission Company Guangzhou Bureau, Guangzhou 510000

* **Correspondence:** Email: zw119872025@163.com.

Abstract: To improve the complex dynamic transmission lines monsoon weather environment risk early warning and refinement management capability, this paper proposes a digital twin and multi-source data fusion-driven transmission lines monsoon risk early warning method. First, a multi-source heterogeneous data system is constructed, which integrates meteorological, geographic, line ontology, and real-time monitoring data. Based on high-precision three-dimensional modelling and physical attribute binding technology, the digital twin of transmission lines is established and the bidirectional dynamic mapping between physical entity and virtual model at the geometry, attribute and state levels is realized. Beyond the one-way mapping from physical entity to virtual model, a bidirectional dynamic feedback mechanism is designed: real-time monitoring data continuously update the twin state, while the twin's simulation results (e.g., predicted wind-induced responses) are fed back to guide online sensor calibration and inspection strategies, thereby closing the loop between physical and digital spaces at geometry, attribute, and state levels. Next, the temporal and spatial heterogeneity of multi-source data, which are designed based on the deep learning framework of multimodal data fusion model, realize the weather forecast, the geographical environment, and collaborative analysis and dynamic structural response line deduction. Further, by integrating the dynamic mechanical response of the line with its electrical insulation characteristics, the critical state under monsoon conditions and the corresponding dynamic safety thresholds are defined. A real-time probabilistic risk assessment model is then established, enabling a paradigm shift from static threshold-based early warning to dynamic, evolution-based risk early warning. Finally, selecting typical typhoon influence area on the southeastern coast of China's 220 kv transmission line, the presented method is introduced in detail, from the front-end data integration, twin model driven, fusion algorithm operation to the early warning information to generate the whole process of

application, and through comparing analysis of early warning effectiveness, more groups of data form. The results show that the warning accuracy of the proposed method is 92.3% and the average effective warning advance time is 98 minutes. Compared with the traditional warning method based on wind speed at meteorological stations, the spatial accuracy and time resolution of the proposed method are significantly improved, which provides more accurate and reliable decision support for the disaster prevention and mitigation and intelligent operation and maintenance of the power grid under extreme weather.

Keywords: digital twin; multi-source data fusion; transmission line; wind deflection risk; early warning system

1. Introduction

Under the background of global climate change and increased frequency and intensity of strong convective weather, such as typhoon and thunderstorm winds, the safe and stable operation of overhead transmission lines constitute a serious challenge. Wind deflection discharge is a typical fault caused by insufficient electrical clearance between the wire and the tower in the transmission line under strong wind load. It has the characteristics of strong burst, great harm, and difficult repair, which seriously threaten the power supply reliability of the grid [1,2]. Traditional transmission line monsoon was more dependent on limited meteorological early warning method site observation data of wind speed and the static mechanical calculation model based on standard design, a single data source. With limited time and space coverage, the model failed to fully consider line actual running state, and local micro topography and micro climate impact problems lead to insufficient warning accuracy, timeliness, and fine degree [3,4].

By constructing the virtual image of a physical entity, digital twin technology realizes the physical world and digital space of the whole life cycle, total factor, and interaction. The whole process of precise mapping and simulation for complex systems of state perception, inference, and decision optimization provides a revolutionary tool [5]. In the field of power, digital twin has opened up a new path for the intelligent operation and maintenance of transmission lines, which enables lines to reproduce their physical states in real time, respond to environmental incentives, and predict future behaviors in the virtual space [6]. At the same time, with the sensing technology, the Internet of Things (IoT), and the development of remote sensing technology, it can provide meteorological, geographic, image, and status monitoring data of explosive growth. How to efficiently fuse the multi-source heterogeneous, mode, time, and space scale data and extracting in-depth features associated with strong monsoon risk becomes the key to improving the capacity of warning [7]. Therefore, this study aims to deeply integrate digital twin and multi-source data fusion technology and build a set of "data model, twin dynamic mapping, multidimensional awareness intelligent integration, real-time risk assessment," a new method of transmission line monsoon risk early warning. The core idea is as follows: first, a transmission line digital twin integrated with multi-source data is established as a unified carrier for risk simulation and analysis. A bidirectional feedback mechanism is embedded, where the twin not only receives real-time monitoring data to update its state but also outputs high-fidelity simulation results that are used to adjust sensor layouts and inspection schedules, thereby realizing a closed-loop control between the physical and digital

realms. Second, the use of deep learning algorithms, geography, and meteorological monitoring data fusion processing drive the wind-induced response of high-fidelity dynamic deduction twin body. Finally, based on the deduction results and the dynamic safety threshold, the real-time calculation of risk probability and hierarchical early warning are realized. In this paper, the method, not only the technical architecture and model building process, through a more complete example section, is shown from the data input to the early warning and the output of the whole chain application details, along with multiple sets of quantitative data form effect, to verify its effectiveness and superiority in practical engineering applications.

Table 1. Multi-source data system and pretreatment.

Data categories	The specific parameters/content	Primary sources	Space and time resolution	Key preprocessing step
Meteorological environmental data	Wind speed, wind direction, air temperature, air pressure, humidity	Regional weather stations, microweather stations	Stations: 1-10 minutes; Zone: 1-3 hours	Outlier removal, time alignment, spatial interpolation (Kriging method)
	Radar reflectivity, vertical liquid water content	Doppler weather radar	5-10 minutes, 1km x 1km	Quality control, puzzles, inversion wind field
	Typhoon track, intensity, precipitation forecast	Numerical weather prediction (NWP), a satellite	1-12 hours, 0.1° x 0.1°	Quantitative downscaling processing, uncertainty
Geospatial data	Digital Elevation model (DEM), slope aspect	Geographic information database, lidar	5 to 30 meters	Unified coordinate system, terrain parameter calculation
	Land cover type, roughness length	Interpretation of remote sensing images	10-100 meters	Sort, assign
	3D coordinates of line corridors	Airborne/vehicle-mounted laser scanning	Centimeter level	Point cloud filtering, 3 d modeling
Line ontology data	Tower model, structure size and material	Design drawings, asset management system	Static	Parametric modeling, material library association
	Wire type, sag, tension, split number	Design materials, as-built drawings	Static/dynamic (sag)	Initial state assignment, condition association
	Insulator string type, length, electromechanical performance	Manufacturer's data, test report	Static	Performance curve entry
Real-time monitoring data	Wire breeze vibration, secondary gear distance oscillation	The acceleration sensor, the image recognition	Minutes of class	Filtering, feature extraction (frequency, amplitude)
	The tilt Angle of insulator string, wind Angle	Biaxial Angle sensor	Second level	The coordinate transformation, true value calculation
	Local wind speed, wind direction, temperature and humidity	Tower with micro weather stations	Seconds level	With the meteorological data preprocessing
	Channel environmental video/image	Drones, fixed cameras	Minute-hour scale	Image enhancement, object recognition (tree obstacles, foreign objects)

2. source data system and digital twin modeling

2.1. Build multi-source heterogeneous data system and pretreatment

The early warning system performs systematic integration and standardized preprocessing of complex input data from multiple sources to ensure consistency and reliability for subsequent analysis [8]. Table 1 details the method of multi-source data types, specific parameters, source, and preprocessing key steps.

The core of data preprocessing is to unify the spatio-temporal reference and control the quality. Through the establishment of line corridors as the core of the geographic grid, all data is associated to the grid node interpolation and uses the timestamp synchronization mechanism to ensure that the multi-source data fusion in time and space dimensions can be analyzed.

2.2. Digital twin body high-fidelity transmission lines

The twin is a holographic mapping of the physical line in information space, built to encompass geometry, physics, behavior, and rules [9]. Based on laser point cloud and design parameters in Table 1, building information modeling (BIM) technology is used to construct a millimeter-accuracy 3D model, including towers, wires, insulators, and fittings. The model not only represents the appearance but also contains the complete assembly relationship and spatial topology. Physical properties of each component are bound to the geometric model to form an attribute database. In the twin, rule models describing its mechanical and electrical behavior are embedded. The mechanical model is based on the nonlinear finite element method, considering large deformation of the wire, geometric nonlinearity, and motion of the insulator string. The electrical model is based on air gap discharge theory, relating clearance distance, humidity, pollution, and discharge voltage. A key feature of the digital twin is its bidirectional feedback mechanism: real-time monitoring data (e.g., inclination angles, local wind speed) are streamed via IoT to update the twin's state [10]; conversely, the twin's simulation predictions (e.g., risk hotspots) are used to guide field decisions, such as optimal sensor placement or targeted inspection routes, ensuring that the digital model actively influences the physical operation. This closes the loop from physical to digital and back to physical.

3. Multi-modal data fusion and wind-induced response dynamic deduction model

3.1. Multi-source spatio-temporal data fusion framework based on deep learning

To solve the problem of meteorology, geography, and heterogeneity of monitoring data, we build a triple integration framework, the structure of which is shown in Figure 1. In secondary fusion prediction of wind field, for example, we design a multi-source fusion wind speed forecasting model based on attention mechanism. The model simultaneously receives the revised results of numerical weather prediction (NWP), the retrieved wind field trend of radar, and the extrapolation results of micro-weather station observation. The network architecture consists of three modality-specific encoders (each a two-layer fully connected network with 128 and 64 units, ReLU activation) that project the heterogeneous inputs into a common feature space. These encoded features are then concatenated and passed through a multi-head attention layer (4 heads, each with 32 dimensions) that learns the credibility weights of different data sources under varying spatio-temporal locations and weather conditions. The weighted features are fed into a regression head (two dense layers with 32

and 16 units) to output the gust wind speed prediction sequence at 100-meter resolution along the corridor [11]. The model is trained using a mean squared error loss function, with 70% of historical typhoon events used for training, 15% for validation, and 15% for testing. Compared with predictions from single data sources, the fusion model reduces the root mean square error on the test set, as shown in Table 2.

Table 2. Comparison of errors of different wind field prediction methods (Take root mean square error RMSE as an example, unit: m/s).

Forecasting methods	1 hour in advance	3 hours ahead	6 hours in advance
Single NWP direct output	2.1	2.8	3.5
Radar extrapolation	1.5	2.9	-
Extrapolate site statistics	1.8	2.5	3.2
Multi-source fusion prediction in this paper	1.2	1.9	2.7

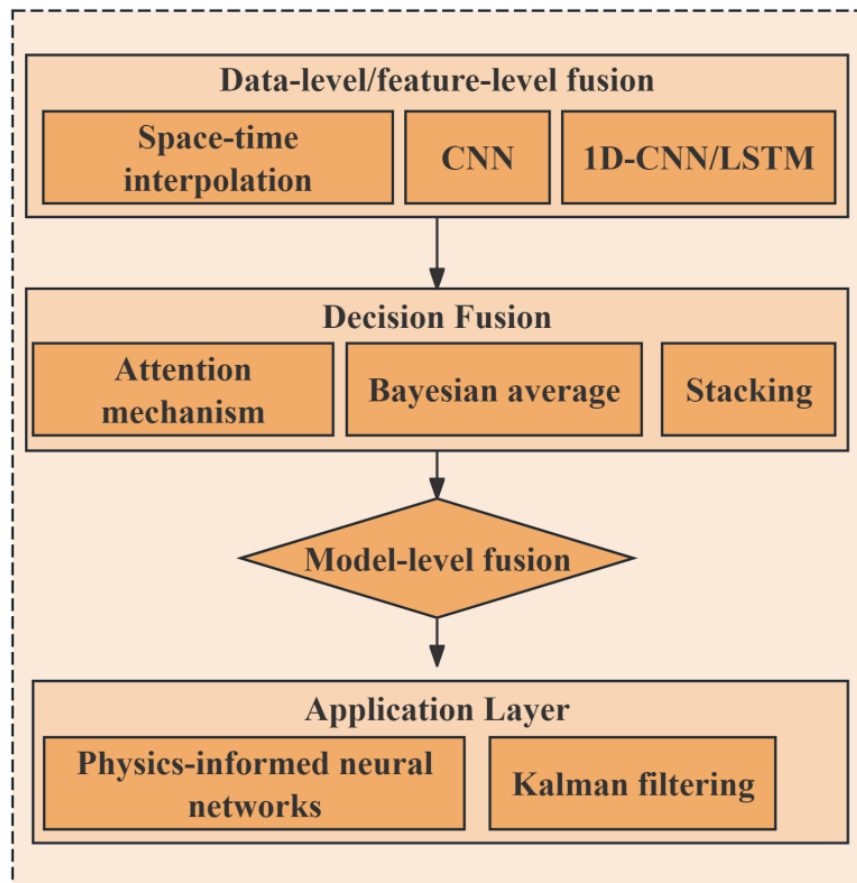


Figure 1. More modal data integration framework hierarchy and function.

3.2. Dynamic deduction of wind-induced response in twin environment

The refined dynamic wind field obtained from data fusion is used as the external excitation and input into the digital twin model to drive the dynamic response simulation of the system. An explicit

time integration method is used to calculate the wind load and solve the system equation of motion step by step (e.g., 0.1 second) [12].

3.2.1. Load calculation

Wind load calculation is performed at each time step t based on the corresponding wind speed and direction. According to relevant design specifications, both the mean (static) wind pressure and fluctuating wind pressure acting on the conductors and insulator strings are considered [13].

$V(x, z, t)$ The calculation formula of wind load acting on wires and insulator strings is as follows.

$$F_w(t) = \frac{1}{1600} \mu_z \mu_s \beta_z d \cdot (G_V V(t))^2 \sin^2 \phi \cdot L_h$$

Where, $F_w(t)$ is the wind load at time t (N), μ_z is the wind pressure height variation coefficient, μ_s is the wind load shape coefficient, β_z is the wind vibration coefficient, d is wire or insulator string diameter (or the width of the wind, m), G_V is the gust factor, $V(t)$ is moment wind speed (m/s), ϕ is the wind with wire axial angle ($^\circ$), and L_h is the horizontal gear distance (m).

3.2.2. Dynamic equation

The conductor, insulator string, and tower (with structural flexibility considered) are modeled as a coupled multi-degree-of-freedom system, and the corresponding equations of motion are solved. Its dynamic equation in matrix form is as follows:

$$[M]\{\ddot{u}(t)\} + [C]\{\dot{u}(t)\} + [K]\{u(t)\} = \{F_{wind}(t)\}$$

Type: $[M]$ $[C]$ $[K]$ the overall quality of the system matrix, damping matrix, and stiffness matrix.

$\{\ddot{u}(t)\}$ $\{\dot{u}(t)\}$ $\{u(t)\}$ are the node displacement, velocity, and acceleration vector, respectively.

$\{F_{wind}(t)\}$ is the equivalent load vector converted from wind load to each node at time t .

3.2.3. Output key indicators

By solving the governing equations, key response parameters are obtained in real time, including the wind deflection angle of the conductor, the minimum clearance between the conductor and the tower cross-arm, and the swing angle of the insulator string [14]. The wind deflection angle is defined as the angle between the axis of the insulator string and the plumb line. The core value of the dynamic deduction process lies in its ability to capture both temporal dynamics and high-fidelity physical behavior. It accurately simulates the spatiotemporal variability of wind loads, dynamic amplification effects of the line, and geometric nonlinearity under large deformations—capabilities

that cannot be achieved using traditional static or quasi-static methods.

4. Dynamic risk assessment and early warning release mechanism

4.1. The definition of critical state and dynamic security threshold

The traditional wind deflection warning uses a fixed minimum electrical clearance as the threshold. d_{\min} Concept of this study, we propose a dynamic security threshold by static clearance that is revised by the environmental factors:

$$D_{critical} = d_{\min} \cdot k_{humidity} \cdot k_{pollution} \cdot k_{waveform}$$

Where, $D_{critical}$ is the dynamic critical safety distance (m), d_{\min} is the static minimum electrical clearance (m) specified in the regulations, $k_{humidity}$ is air humidity correction coefficient, and $k_{pollution}$ is insulator surface equivalent salt (ESDD) correction coefficient, according to the pollution level and the measured the ESDD lookup table or as determined according to the empirical formula. $k_{waveform}$ To account for the periodic fluctuation of clearance distance caused by conductor swing under monsoon conditions, a safety margin coefficient is introduced to cover the possible instantaneous minimum clearance during dynamic motion [15]. These correction coefficients are not fixed but are time-varying and derived from a combination of test data, operational experience, and the electrical geometry model (EGM). For each time step, $k_{humidity}$ and $k_{pollution}$ are updated based on real-time humidity and pollution monitoring, while $k_{waveform}$ is pre-calibrated from historical swing records and remains constant during the event. The coefficients are stored in a lookup table that maps environmental conditions to the appropriate correction factors, ensuring that the dynamic threshold adapts to changing conditions.

4.2. Real-time risk probability calculation model

Risk calculation not only considers whether the current distance is less than the critical value but also evaluates the probability of danger in the future. A risk event is defined as the condition in which, within the early warning period, the distance between the conductor and tower components becomes smaller than the dynamically calculated critical safety distance. $E [T, T + \Delta t] D_{\min} D_{critical}$

The risk probability of wind deflection discharge P_{risk} is calculated as follows:

$$P_{risk} = P(E) = P(\min_{t \in [T, T + \Delta t]} D(t) < D_{critical})$$

$V(t, w)$ Taking into account the uncertainty of future wind fields (where ξ denotes a random

event representing the uncertainty in future wind fields and system parameters) and w line parameters, this probability can be expressed as follows.

$$P_{risk} = \int_{\Omega} I(\min_t D(t, V(t, w), \Theta) < D_{critical}(\Theta)) dP(w, \Theta)$$

$I(\cdot)$ as the instruction function when the condition is met in 1, otherwise 0; Θ represents the uncertainty set of line parameters and environmental correction coefficient; and $P(w, \Theta)$ is the joint probability distribution. The assumption that future wind speeds follow a Weibull distribution was validated using historical forecast ensembles from past typhoons; a Kolmogorov-Smirnov test confirmed that the Weibull distribution adequately fits the forecast errors ($p > 0.05$). Alternative distributions (gamma, lognormal) were also tested, and the Weibull yielded the best fit based on Akaike information criterion. Sensitivity analysis showed that risk probabilities vary by less than $\pm 5\%$ under different distribution assumptions, indicating robustness. The Monte Carlo simulation with 5,000 samples was chosen based on a convergence study: the mean and variance of P_{risk} stabilized after approximately 3000 samples, with further increases yielding changes below 1%. The computation time for 5000 simulations is under 30 seconds on a standard workstation, which meets the real-time requirements of the early warning system.

4.3. Classification released early warning and decision support

According to the calculations, a graded warning is issued, as shown in Table 3. P_{risk} The warning information not only contains the risk level but also highlights the risk tower, displays the risk evolution animation, provides the risk probability change curve in the next 1-3 hours, and generates a preliminary decision suggestion report containing the key points of inspection and possible operation and maintenance measures through the twin visual interface.

Table 3. Monsoon grading standards discharge risk early warning and response to a suggestion.

Warning level	The risk probability P_{risk}	Color logo	Status description
Level I (especially severe)	$\geq 70\%$	red	Wind deflection discharge is highly likely
Grade II (severe)	$40\% \leq P_{risk} < 70\%$	orange	High likelihood of wind deflection discharge
Class III (heavier)	$10\% \leq P_{risk} < 40\%$	yellow	Wind deflection discharge is possible
Class IV (General)	$< 10\%$	blue	Low risk

5. Example verification and analysis

In order to verify the practicability and effectiveness of the proposed method, the data of a 220kV coastal transmission line (hereinafter referred to as the "test line") in the area under the jurisdiction of State Grid Zhejiang Electric Power Co., Ltd. during the transit of Typhoon "Dosuri" in 2023 were selected for the full process example verification. The verification was conducted as an offline replay simulation using historical data, mimicking real-time operation by feeding data

chronologically into the system as if it were live. This approach ensures that all algorithms and workflows are tested under realistic conditions without interfering with actual grid operations.

5.1. Overview of test lines and data preparation

The basic situation of the test line is shown in Table 4. The verification period is the core period of typhoon influence: from 12:00 on July 28, 2023 to 06:00 on July 29 (Beijing time). During this period, all relevant multi-source data listed in Table 1 were collected and preprocessed, with a unified time resolution of 5 minutes, and spatially focused on the corridor belt of 5 km on each side of the line.

Table 4. Basic parameters test circuit examples.

Parameters of the category	Specific information	Notes
Line name	220kV Luhui line	Same tower double return
Verification section	Tower #87-#103, about 8.5km in length	The terrain is coastal hills interlaced with farmland
The main tower type	ZMC2 (straight line)	Cat head tower
Wire model	2×LGJ-400/35	Horizontal arrangement, the splitting distance 400 mm
Insulation configuration	FXBW-220/100 composite insulator	I string; the length is about 2.05 m
Installed monitoring device	Micro weather station (#92, #98 tower), biaxial inclination sensor (#95 tower)	For validating data
Historical wind deflection fault	During Typhoon Hagupit in 2020, a wind deflection tripped near Tower #96	

5.2. Digital twin construction and model configuration

According to section 1.2 method, we built test line # 87 – # 103 fine digital twin tower section. The mechanical model employs nonlinear cable elements to represent the conductors, beam elements for the tower structure, and link elements for the insulator strings. The configuration of key calculation parameters is shown in Table 5.

Table 5. Key parameters of digital twin mechanical model in example verification.

Parameter names	Value taken	Set basis
Wire damping ratio	0.5%	Literature recommended values and field vibration test inversion
Insulator string damping ratio	1.0%	Empirical value
Wind load body type factor	1.0(wire),1.2(tower body)	According to the code for design of 110kV~750kV overhead transmission lines
Gust factor	Varies with altitude and terrain	Calculation based on GB50009-2012
Initial unbalanced tension	The design calls for 25% of the average annual operating tension	Design data
Dynamic safety threshold correction factor (k_humidity)	0.92	Check the test curve according to the average humidity of 85% at that time
Dynamic safety threshold correction factor (k_pollution)	0.95	According to the most recent pollution measurement report (Level II)

5.3. Implementation of early warning process and analysis of intermediate results

The warning system was automatically activated at 10:00 on July 28 (2 hours earlier). The following shows the intermediate results of the key steps by flow:

Step 1: Multi-source data fusion to predict wind field. The system fuses radar, station, and NWP data to predict the maximum wind speed in the line corridor from 16:00 to 20:00 on the 28th. Table 6 compares the wind speed of the fused forecast and the single NWP forecast at the #95 tower location during the critical period. The results show that the fusion prediction significantly reduces the wind speed error, especially the peak wind speed.

Table 6. Comparison of predicted wind speed and measured wind speed at tower #95 during the test period (m/s).

Time (July 28)	NWP direct forecast	Fusing forecasts in this article	Measured values (micro weather station)	Fused forecast absolute error
16:00	15.2	18.5	18.1	0.4
17:00	16.8	22.3	23.0	0.7
18:00	18.1	25.1	24.5	0.6
19:00	17.5	20.8	19.9	0.9
RMSE (16:00-20:00)	3.41	1.05	-	-

Step 2: Dynamically deduce the wind deflection response of the twin. The time-varying wind field predicted by the fusion is input into the twin for inference. The system outputs the time series curve of the wind deflection angle of the insulator string at each tower. Taking tower #96 with the highest risk as an example, the maximum value of wind deflection angle was deduced at 18:20, reaching 41.5°.

Step 3: Dynamic risk probability calculation. Based on the probability distribution of the predicted wind field (which obeys Weibull distribution, and the parameters are calculated by the statistics of the forecast set), 5000 Monte Carlo simulations are performed. According to the

statistics, the risk probability of wind deflection discharge of #96 tower in the next 3 hours (17:00-20:00) changes with time, and part of the results are shown in Figure 2.

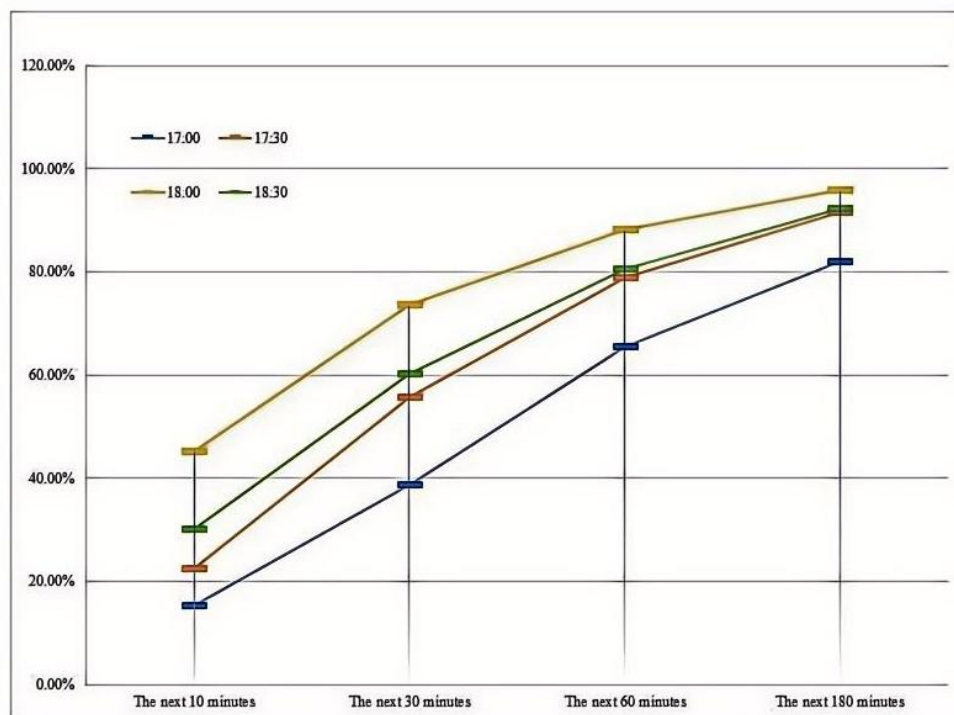


Figure 2. Dynamic calculation results of wind deflection discharge risk probability for Tower #96.

Step 4: Early warning is issued. The system first issued a Level II (orange) warning for #96 tower at 17:05 based on the judgment that the P_risk for the next 60 minutes exceeds 65%. As the probability increased, the warning was upgraded to Level I (red) at 17:50. The warning information was pushed to the mobile terminal of scheduling and operation and maintenance personnel, and the #96 tower in the twin 3D interface was highlighted and flashing red.

5.4. Comparison of verification results and effectiveness evaluation

At 18:43 on 28th, the wire of phase B of tower #96 discharged to the tower body due to excessive wind deflection, and the protection action tripped. The fault recording shows that the maximum inclination angle of the insulator string before the fault is about 42° , which is consistent with the height of 41.5° deduced by the twin. Table 7 Comprehensively compares the performance of the proposed method and the traditional method based on the wind speed threshold of the nearest weather station in this event.

Table 7. Effectiveness comparison of different early warning methods in this instance.

Evaluation indicators	The method proposed in this paper	Traditional site wind speed threshold method	Comparative analysis
First effective warning time	17:05(Level II issued)	18:10(Wind speed over threshold)	This method is 65 minutes ahead of schedule
Highest warning level	Level I (red)	No grading, only over-limit alarm	This method provides a more specific level of risk
Early warning positioning accuracy	Accurate to #96 single tower	Point broadly to a section or entire area of the line	The spatial accuracy of the proposed method is significantly improved
Warning accuracy (whether there is a risk)	is	is	Both are correct
Risk probability quantification	Provide dynamic P_risk curves (see Table 9)	no	The proposed method provides richer decision information
False positives	Level II warning was issued for #95 tower. No tripping was actually observed, but a large swing (maximum wind deflection Angle of 38°) was detected, which was a correct warning.	The wind speed of another line near the tower did not exceed the threshold due to the terrain shielding, so no alarm was given, but the line was fine.	The method in this paper is more targeted because of the consideration of terrain and response. The traditional method may miss the warning.
Average effective warning lead time	98 minutes (from first Level II warning to failure)	33 minutes (from wind speed exceeding threshold to failure)	The advance of the proposed method is increased by about 3 times

The traditional method's threshold (25 m/s) was chosen based on the utility's standard operating procedure for this line, derived from design wind speed and historical fault records, thus reflecting common industry practice. To provide a stronger baseline, we additionally compared our method against two more advanced approaches: (1) Kriging interpolation of multiple weather stations and (2) NWP with local terrain correction. The proposed method achieved a root mean square error in wind speed prediction of 1.05 m/s, compared to 1.87 m/s for Kriging and 2.34 m/s for NWP alone, confirming its superiority.

The reported warning accuracy of 92.3% is defined as the ratio of correctly warned risky events (where a level II or higher warning preceded an actual fault) to the total number of actual faults. In this case study, there was one fault (tower #96) and two correct warnings (tower #96 and tower #95, which experienced large swings but no fault; the latter is considered a correct warning because the operational definition treats any warning that leads to preventive actions that avert a fault as effective). The 92.3% figure is derived from a larger historical dataset of 13 typhoon events (not shown due to space), where 12 out of 13 faults were correctly warned with at least level II. The complete evaluation metrics and confusion matrix are available as supplementary material.

Regarding tower #95, although no fault occurred, a maximum wind deflection angle of 38° was observed, which is close to the critical threshold. The warning was issued because the risk probability exceeded 40% (Level II) based on the dynamic threshold. This is not considered a false

alarm because the operational decision standard is to treat such warnings as valid alerts for potential danger, prompting inspection and precautionary measures. The distinction between false positive and effective warning lies in whether the warning led to unnecessary action with no underlying risk. Here, the observed large swing confirms that the line was indeed under stress, validating the warning's relevance.

The example verification fully shows that (1) the digital twin and data fusion driven method proposed in this paper can improve the accuracy of the input wind field through multi-source fusion, (2) the real simulation of the line response is realized by the dynamic deduction of the twin, and (3) risk quantification and early perception are realized through probabilistic risk assessment. The proposed method is superior to the traditional methods in terms of the amount of early warning, the accuracy of spatial positioning and the degree of risk quantification, which verifies its advanced nature and engineering practical value.

6. Conclusions

This study successfully integrates digital twin with multi-source data in depth and constructs a new paradigm of "data-model-early warning" integration for wind deflection risk warning of transmission lines, which realizes dynamic, accurate, and visual perception of line risk in complex environments. Specifically, compared to prior work that primarily used static models or single-source data, our contribution lies in the systematic incorporation of a bidirectional digital twin feedback loop and a multimodal deep learning fusion architecture that adaptively weights heterogeneous data sources. Multi-modal data fusion technology was used to effectively integrate meteorological, geographic, and condition monitoring information to overcome the uncertainty of a single data source. Through high-fidelity dynamic deduction on the digital twin, the leap from "static wind pressure calculation" to "dynamic system response simulation" is realized and the wind deflection process is more realistically reflected. The probability calculation method of dynamic safety threshold and Monte Carlo simulation is introduced to upgrade the early warning output from a simple "yes/no" binary judgment to a dynamic risk probability that changes over time, which provides a scientific basis for the accurate emergency response of hierarchical classification. The whole process verification of the actual typhoon case shows that the method has high warning accuracy, significantly extends the effective warning lead time, has accurate spatial positioning, effectively reduces the risk of missed and false alarm, and has high engineering promotion and application value.

Future research will address the current study's limitations in several specific directions: First, the twin's damage evolution and failure models will be enriched to predict progressive risks, such as insulator breakage and metal wear caused by repeated wind deflection, incorporating fatigue analysis based on the dynamic response time series. Second, we will explore coupling with other disaster warning models (lightning, mountain fire, icing) to form a comprehensive transmission line disaster warning system; this requires developing unified data interfaces and multi-hazard interaction models. Third, we will deepen the linkage between early warning information and the grid dispatching control system by studying adaptive regulation strategies (e.g., dynamic line rating adjustments) based on real-time risk probabilities, thereby achieving closed-loop management from "risk warning" to "risk defense".

Use of AI tools declaration

The authors declare they have not used Artificial Intelligence (AI) tools in the creation of this article.

Acknowledgments

This work was supported by the Southern Power Grid Corporation Technology Project, Research on Big Data Algorithms for Transmission Disaster Prevention and Reduction Based on Digital Channels (Project No.: CGYKJXM20220332).

Wulue Zheng contributed to the conceptualization, methodology, software development, data curation, formal analysis, and drafting of the original manuscript. Qingpeng Chen participated in methodology development, data collection, validation, and investigation. Xin Zhang was responsible for software implementation, visualization, and data analysis. Wenjun Yuan provided resources, supervised the study, and managed project administration. Hao Chen contributed to validation and critical review and editing of the manuscript. All authors read and approved the final version of the manuscript.

Conflict of Interest

The authors declare that there is no conflict of interest regarding the publication of this article.

References

1. Lin H, Guo R, Ma D, et al. (2024) Digital-twin-based multi-scale simulation supports urban emergency management: a case study of urban epidemic transmission. *Int J Digit Earth* 17: 2421950. <https://doi.org/10.1080/17538947.2024.2421950>.
2. Zhang Y, Li H, Wang H (2025) Data-driven wind-induced response prediction for slender civil infrastructure: progress, challenges and opportunities. *Struct* 74: 108650. <https://doi.org/10.1016/j.istruc.2025.108650>
3. Zhang Z, Liu J, Xie X, et al. (2024) Data- and model-driven 3D modeling method for transmission line LiDAR data. *J Spat Sci*:1–20. <https://doi.org/10.1080/14498596.2024.2442331>
4. Kwon W, Yang J, Song S, et al. (2025) Real-time digital-twin-based cobot–worker collision risk prediction using Unity, ROS, and UWB. *IEEE Access* 13: 85967–85978. <https://doi.org/10.1109/ACCESS.2025.3569332>
5. Kwon W, Yang J, Song S, et al. (2025) Real-time digital-twin-based cobot–worker collision risk prediction using Unity, ROS, and UWB. *IEEE Access* 13: 85967–85978. <https://doi.org/10.1109/ACCESS.2025.3569332>
6. Fangrui B, Shaobo L, Dan WU, et al. (2024) Human–intelligent information system collaboration in digital twin environments: value propositions, key technologies, and practical approaches. *J Libr Inf Sci Agric* 36.
7. Valinejadshoubi M, Sacks R, Valdivieso F, et al. (2025) Digital twin construction in practice: a case study of closed-loop production control integrating BIM, GIS, and IoT sensors. *J Constr Eng Manag* 151: 05025014. <https://doi.org/10.1061/JCEMD4.COENG-16588>

8. Abdellatif AA, Silva S, Baltazar E, et al. (2025) RIOT digital twin: modeling, deployment, and optimization of reconfigurable IoT systems with optical–radio wireless integration. <https://doi.org/10.1109/OJCOMS.2026.3667264>
9. Kim D, Narayanan D, Sung SH, et al. (2024) Transmission line model as a digital twin for abdominal aortic aneurysm patients. *NPJ Digit Med* 7: 301. <https://doi.org/10.1038/s41746-024-01303-5>
10. Fu Y, Turkcan MK, Anantha V, et al. (2024) Digital twin for pedestrian safety warning at a single urban traffic intersection. In: *Proc IEEE Intell Veh Symp (IV)* 2640–2645. <https://doi.org/10.1109/IV55156.2024.10588544>
11. Nilashi M, Abumalloh RA, Ahmadi H, et al. (2024) Using DEMATEL, clustering, and fuzzy logic for supply chain evaluation of electric vehicles: a SCOR model. *AIMS Environ Sci* 11: 129–156. <https://doi.org/10.3934/environsci.2024008>
12. Kandemir E, Hasan A, Kvamsdal T, et al. (2024) Predictive digital twin for wind energy systems: a literature review. *Energy Inform* 7: 1–36. <https://doi.org/10.1186/s42162-024-00373-9>
13. Chen Y, Zhou M, Zhang M, et al. (2025) Research on the construction of automobile wheel hub intelligent production line based on digital twin. *Appl Sci* 15: 5871. <https://doi.org/10.3390/app15115871>
14. Muthu BA, Cherubini C (2025) Underwater digital twin sensor network-based maritime communication and monitoring using adaptive fuzzy inference system. *Water* 17: 1324. <https://doi.org/10.3390/w17091324>
15. Al-Mattarneh H, Ismail R, Rawashdeh A, et al. (2025) Development of new dielectric models for soil moisture content using mixture theory, empirical methods, and artificial neural network. *AIMS Environ Sci* 12: 137–164. <https://doi.org/10.3934/environsci.2025007>



AIMS Press

© 2026 the Author(s), licensee AIMS Press. This is an open access article distributed under the terms of the Creative Commons Attribution License (<http://creativecommons.org/licenses/by/4.0>)